Atmospheric Environment 125 (2016) 461–473

Contents lists available at ScienceDirect

Atmospheric Environment

journal homepage: www.elsevier.com/locate/atmosenv

Aerosol characteristics in north-east India using ARFINET spectral optical depth measurements

B. Pathak[a,*], T. Subba[a], P. Dahutia[a], P.K. Bhuyan[a], K. Krishna Moorthy[b], M.M. Gogoi[c], S. Suresh Babu[c], L. Chutia[a], P. Ajay[a], J. Biswas[a], C. Bharali[a], A. Borgohain[d], P. Dhar[e], A. Guha[e], B.K. De[e], T. Banik[e], M. Chakraborty[e], S.S. Kundu[d], S. Sudhakar[d], S.B. Singh[f]

[a] Centre for Atmospheric Studies, Dibrugarh University, Dibrugarh 786 004, India
[b] Indian Space Research Organization Head Quarters, Antariksh Bhavan, New BEL Road, Bengaluru 560 231, India
[c] Space Physics Laboratory, Vikram Sarabhai Space Centre, Thiruvananthapuram 695 022, India
[d] North-East Space Application Centre, Umiam, Shillong, Meghalaya 793 103, India
[e] Department Physics, Tripura University, Agartala 799022, India
[f] Department of Physics, Manipur University, Imphal 795003, India

HIGHLIGHTS

- Aerosol characteristics in the North-East India exhibits a west to east gradient.
- Aerosol loading in the North-East India ranks second highest in Asia next to IGP.
- Surface forcing and consequent atmospheric heating exceeds many locations of India.
- Elevated aerosol layers are caused by upper air transportation.

ARTICLE INFO

Article history:
Received 18 February 2015
Received in revised form 28 July 2015
Accepted 29 July 2015
Available online 4 August 2015

Keywords:
Aerosol optical depth
Multiwavelength solar Radiometer
ARFINET
Ångström exponent
Extinction coefficient
HYSPLIT
Aerosol radiative forcing

ABSTRACT

Four years (2010–2014) of spectral aerosol optical depth (AOD) data from 4 Indian Space Research Organisation's ARFINET (Aerosol Radiative Forcing over India) stations (Shillong, Agartala, Imphal and Dibrugarh) in the North-Eastern Region (NER) of India (lying between 22–30°N and 89–98°E) are synthesized to evolve a regional aerosol representation, for the first time. Results show that the columnar AOD (an indicator of the column abundance of aerosols) is highest at Agartala (0.80 ± 0.24) in the west and lowest at Imphal (0.59 ± 0.23) in the east in the pre-monsoon season due to intense anthropogenic biomass burning in this region aided by long-range transport from the high aerosol laden regions of the Indo-Gangetic Plains (IGP), polluted Bangladesh and Bay of Bengal. In addition to local biogenic aerosols and pollutants emitted from brick kilns, oil/gas fields, household bio-fuel/fossil-fuel, vehicles, industries. Aerosol distribution and climatic impacts show a west to east gradient within the NER. For example, the climatological mean AODs are 0.67 ± 0.26, 0.52 ± 0.14, 0.40 ± 0.17 and 0.41 ± 0.23 respectively in Agartala, Shillong, Imphal and Dibrugarh which are geographically located from west to east within the NER. The average aerosol burden in NER ranks second highest with climatological mean AOD 0.49 ± 0.2 next to the Indo-Gangetic Plains where the climatological mean AOD is 0.64 ± 0.2 followed by the South and South-East Asia region. Elevated aerosol layers are observed over the eastern most stations Dibrugarh and Imphal, while at the western stations the concentrations are high near the surface. The climate implications of aerosols are evaluated in terms of aerosol radiative forcing (ARF) and consequent heating of the atmosphere in the region which follows AOD and exhibit high values in pre-monsoon season at all the locations except in Agartala. The highest ARF in the atmosphere occurs in the pre-monsoon season ranging from 48.6 Wm^{-2} in Agartala to 25.1 Wm^{-2} in Imphal. Winter radiative forcing follows that in pre-monsoon season at these locations. The heating rate is high at 1.2 K day^{-1} and 1.0 K day^{-1} over Shillong and Dibrugarh respectively in this season. However, Agartala experiences higher surface forcing (−56.5 Wm^{-2}) and consequent larger heating of the atmosphere of 1.6 K day^{-1} in winter.

* Corresponding author.
E-mail address: Pathak.binita8@gmail.com, binita@dibru.ac.in (B. Pathak).

http://dx.doi.org/10.1016/j.atmosenv.2015.07.038
1352-2310/

1. Introduction

The rapid socio-economic development in the recent past has increased the anthropogenic emissions in the South Asian region along with several other parts of the world. The South Asian and East Asian regions, comprising of the Indian mainland, Bangladesh, Myanmar and the vast Chinese mainland are among the potential sources of a variety of aerosol species; both natural and anthropogenic, and extensive investigations are being made in the past years (e.g., Chin et al., 2000; Girolamo et al., 2004; Moorthy et al., 2013). These densely populated regions are also vulnerable to the impacts of atmospheric aerosols and traces gases, through climate change, regional air quality degradation and human health (e.g., Liu et al., 2009). To better understand and investigate atmospheric aerosols and their impact on climate in this region apart from ground based networks such as Aerosol Robotic Network (AERONET) (Holben et al., 1998), Sky Radiometer (SKYNET) (Nakajima et al., 2003), Aerosols Radiative Forcing over India NETwork (ARFINET) (Moorthy et al., 2013; Babu et al., 2013) etc., several research campaigns like the Indian Ocean Experiment (INDOEX), Aerosol Characterization Experiment-Asia (ACE-Asia), Pacific Exploratory Mission (PEM) A (1991) and B (1994), Transport and Chemical Evolution over the Pacific (TRACE-P), Atmospheric Particulate Environment Change Studies (APEX) and Atmospheric Environmental Impacts of Aerosols in East Asia (AIE), Pacific Exploration of Asian Continental Emission (PEACE), East Asian Regional Experiment (EAREX) 2005, ABC Maldives Monsoon Experiment (APMEX), Integrated Campaign for Aerosols, gases and Radiation Budget in Pre-monsoon (ICARB) and Winter seasons (W_ICARB), Regional Aerosol Warming Experiment (RAWEX) etc. have been conducted particularly in the Indo-Asia-Pacific region (Nakajima et al., 2007 and references therein; Takami et al., 2007 and references therein; Moorthy et al., 2008, 2010; Babu et al., 2011). Few major findings of these studies are: Asia with AOD ~0.36 is ranking second highest in aerosol burden in the world next to Africa as revealed by AERONET measurements (Li et al., 2007 and references therein), statistically significant increasing trend of aerosol optical depth in Indian subcontinent (~2.3% yr^{-1}) with considerable contribution from anthropogenic fraction and increasing atmospheric warming by aerosol absorption in the elevated aerosol layers over the Indian landmass as revealed by ARFINET measurements, contribution of anthropogenic aerosols on surface diming and atmospheric heating as well as on cloud formation as revealed by INDOEX. Moreover, the optical properties of Asian mineral dust-enriched aerosols look much different from that of other arid regions such as that of Saharan dust plumes, Asian aerosols are mixture of anthropogenic air pollutants and mineral dust in the spring season, contribution of aerosols to the suppression of precipitation and the slowdown of hydrological cycles by dust storms, to air pollution and to fire smoke plumes, larger reduction of the solar radiation budget at the surface than at the top of the atmosphere due to absorbing aerosols and strong radiative heating in the atmosphere due to the mixing state of black carbon etc are some other findings (Li et al., 2004 and references therein).

The Himalayan foothill regions have a special importance in this context. In the regional characterization of aerosols over south Asia, a study from the eastern Himalayan foothill region covering the North-Eastern part of India (NER) assumes significance owing to differences in aerosol sources, varying from the background continental aerosols to secondary biogenic aerosols emitted by the huge forest cover (66%) to anthropogenic biomass burning, industrial (oil wells, gas fields, coal mines, brick klins etc.) and vehicular emissions. In addition to its geographical position, being surrounded by East Asia, South-East Asia, China and the mainland of India, the characteristic dense vegetation, vast water bodies, heavy rainfall pattern and the unique topography and exposure to densely populated Indo-Gangetic plains towards the west (which makes the region prone to heavy external influence) results in a complex aerosol environment in NER. The blocking by mountains all around and convergence effects over the foothills of the Himalayas over NER produces favourable conditions for the accumulation of both remote and local aerosols establishing a sharp regional gradient. This region is conducive for troposphere–stratosphere exchange of atmospheric constituents including aerosols and gases. Li et al. (2005) from chemical transport model analysis have demonstrated how the boundary layer pollutants from NER and South-West China could be transported and orographically lifted to the upper troposphere over South Asia and are trapped by the Tibetan Plateau anticyclone. According to Bonasoni et al. (2010) the southern side of the high Himalayan valleys represent a “direct channel” able to transport pollutants up to 5 km above sea-level, where the pristine atmospheric composition can be strongly influenced, especially during the pre-monsoon season. This is consistent with the observation of enhanced aerosol optical depth (AOD) and black carbon concentration in pre-monsoon season over the pristine elevated Himalayan regions (Babu et al., 2011; Dumka et al., 2011; Gogoi et al., 2014). The enhanced deposition of absorbing aerosols over the snow and glaciers result in regional radiative forcing through direct and snow albedo forcing over the Himalayan regions (e.g., Krinner et al., 2006) adding to the vulnerability. This region is also found to support new particle formation from pre-cursors (Moorthy et al., 2011; Kompalli et al., 2014).

Several studies, based on long term database as well as campaigns, have been performed over western part of Himalayan foothills including the IGP in the recent years; however, extensive studies on aerosols in the eastern part of IGP and the eastern Himalayan foothills (i.e., NER) are virtually non-existent, except few isolated works form Dibrugarh and Darjeeling (Pathak et al., 2010, 2012; Adak et al., 2014) and short campaigns (Pathak et al., 2014; Rahul et al., 2014). These studies have recognized the pre-monsoon (March–May), as the season heavily loaded by column aerosols in Dibrugarh which results in the highest seasonal aerosol radiative forcing and consequent heating of the atmosphere. On the other hand, aerosol loading within the atmospheric boundary layer maximizes in winter, indicating heterogeneity between surface and column aerosol loading over the location and thereby demonstrating the existence of elevated aerosol layer. These studies have also established the influence of transported aerosols originating from different regions of India and west Asia and traversing Indo Gangetic Plains (IGP) and finding the way through the western corridor towards the Brahmaputra valley. Babu et al. (2013) has accounted a strong increasing trend of aerosols over Dibrugarh during last decade. The land campaigns revealed the spatial heterogeneity of particulate matter and Black Carbon (BC) aerosols across the Brahmaputra Valley of North-East India (Pathak et al., 2014) and also the presence of elevated BC layer in monsoon season (Rahul et al., 2014). As per few observations (e.g., Cao et al., 2010) Tibetan plateau and south China are affected by pollutants transported from the NER. However, systematic reports on extensive investigation on aerosol abundance and characteristics are still absent from locations other than Dibrugarh (Pathak et al., 2014 and references therein) and from Agartala (Guha et al., 2015).

In this paper we present the spatial and temporal distinction of optical and physical parameters (AOD, extinction coefficient, Ångström Exponent or size distribution) during 2010–September 2014 for the four ARFINET stations in NER: Dibrugarh (DBR), Imphal (IPH), Shillong (SHN), and Agartala (AGA) (Fig. 1). This is expected to derive a regional picture of aerosols and their impact on climate and environment in the NER for the first time in Asian aerosol domain. As such, the regional features are compared with those reported from other locations/regions in South, South-East

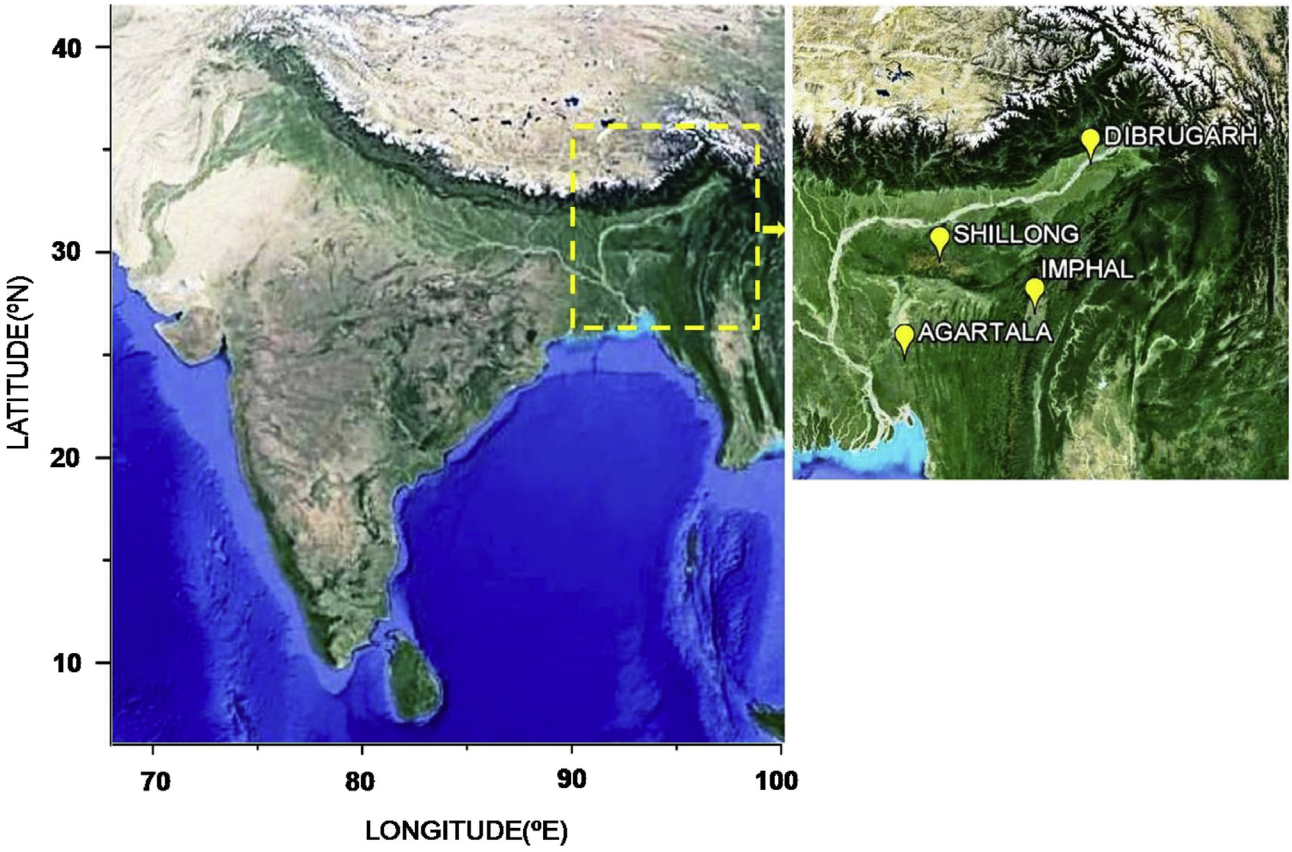

Fig. 1. Map of India showing the study locations in North-Eastern Region of India. The dashed box represents the region covering the study locations marked with yellow symbol in the other figure. (For interpretation of the references to colour in this figure legend, the reader is referred to the web version of this article.)

and East Asia. An attempt has also been made to investigate the implications of aerosol by estimating aerosol radiative forcing and consequent heating in the atmosphere of the region. This work will be helpful in understanding the aerosol effect on regional climate in the South Asia and can eventually help in assessing the effect of aerosol dynamics on Indian summer monsoon.

2. Study region, meteorology and database

2.1. Study region: NER

The NER, one of the 34 biodiversity hotspots in the world, stretches between 22°N and 30°N latitude and 88°E and 98°E longitude and occupies a special position in the geography of the Indian monsoon region. Nestled between the eastern Himalayas, Tibetan Plateau in the north, the Indo Myanmar range of hills in the east, IGP and Bangladesh in the west and south-west this region comprises of the states of Arunachal Pradesh, Assam, Manipur, Nagaland, Meghalaya, Mizoram, Sikkim and Tripura with about 72% area under hilly ecosystem. Rocky surface, alpine vegetation and snow-capped high peaks dominate the physical landscape of this area. The region receives highest rainfall every year during June–August and this has made the region to be clothed with diverse and dense vegetation. Bio-mass burning, especially as a part of shifting cultivation is widely prevalent in this region and it, along with brick kilns (coal-fired) and oil and gas fields makes this region vulnerable to anthropogenic emissions. It is found that the average sulphur content in coal here ranges from 2 to 4%, which is comparable to that of the Chinese coal and exceeds the Indian average by is 4–8%. The emissions from the coal based coke oven industries have a significant impact on the concentration of particulate matter, SO_2, volatile organic compounds (VOCs) and trace metals like Te, Mn, V, Co, Ni, Zn, Mo, Cd, Sn etc. over the region (e.g., Khare and Baruah, 2010).

The measurement sites (Fig. 1) bear unique environmental and topographic characteristics. DBR a major city in eastern India with population density 393 km^{-2} and situated in the upper Brahmaputra basin is the emerging communication, healthcare and industrial hub of NER. It is known as the 'Tea city in India' with large number of tea gardens. IPH the capital city of Manipur state is located south of DBR in the south-eastern part of the region close to the Indo-Myanmar boarder and is having a population density of 640 km^{-2}. AGA, the capital of the Indian state of Tripura is the second largest city in NER after Guwahati, both in municipal area as well as population (density 5730 km^{-2}). AGA lies in a plain on the bank of the Haora River and is located 2 km from the border of heavily populated and polluted Bangladesh. SHN, located in the centre of the Shillong Plateau is surrounded by hills. It is the capital city of Meghalaya province with population density of 234 km^{-2} and is just 55 km from Mawsynram, the world's wettest place. The measurement site here is ~20 km downwind of the Shillong city.

2.2. Prevailing meteorology

The weather and climate over NER is significantly influenced by the interaction between large scale circulation and the local topography. The region exhibits typical tropical weather pattern with mild, cool, dry and relatively short winter (December–February), hot and humid pre-monsoon (March–May) and extended rainy sea-

sons. In the monsoon (June–September), the region experiences heavy rain on almost a daily basis. The annual variation of monthly total rainfall at the four locations is shown in Fig. 2(a) in top 4 panels, while bottom two panels depict the monthly mean maximum and minimum temperatures as well as relative humidity (RH). SHN receives highest monsoon rainfall, and AGA is the warmest and most humid location. Synoptic wind pattern at 850 hPa level generated using Weather Research Forecast (WRF)-Meteorology is primarily calm north-easterly during winter and retreating monsoon (October–November) seasons and calm westerly in pre-monsoon (Fig. 2(b)). The winds drastically change to moderate to strong south-westerlies in monsoon.

2.3. Data and methodology

2.3.1. Aerosol optical depth and Ångström wavelength exponent

Spectral aerosol optical depth (AOD) has been estimated regularly at all the stations on clear and partly cloudy (when the solar disc and the region ~10° around it are cloud free) using the Multi-Wavelength solar Radiometer (MWR) and the Microtops-II sun photometer (MTOP) as detailed in Table 1. In the station SHN, MTOP AOD has been used whenever MWR AOD is unavailable.

MWR provides AOD at 380, 400, 450, 500, 600, 650, 750, 850, 935 and 1025 nm. MTOP attached with a GPS measures instantaneous AOD at 5 of the eight wavelengths; 380, 440, 500, 675, 870, 936 and 1020 nm depending on the model (Moorthy et al., 1997; Bhuyan et al., 2005; Gogoi et al., 2009). The wavelength range for the MTOP in AGA and IPH is 380–870 nm while in SHN the last two wavelengths are 936 and 1020 nm instead of 675, 870. It is pertinent to mention that the 935 or 936 nm wavelength in both MWR and MTOP is greatly affected by water vapour absorption and is used to measure water vapour content. Langley technique is used to derive the spectral AOD in both the instruments. Details on MWR and MTOP are available in several earlier reports (e.g., Moorthy et al., 2007; Gogoi et al., 2009; Morys et al., 2001; Moorthy et al., 2010). Typical errors in AOD measurements from MTOP are ~0.03 (Morys et al., 2001) and from MWR is 0.02–0.03 at different wavelengths (Gogoi et al., 2009). The frequency of operation for MWR is daily and under clear sky condition, during a day we can get separate AOD data set for forenoon and afternoon. The MTOP is operated on an hourly/half hourly basis for 3–4 days in a week under the clear sky condition. Data for the period October 2010–September 2014 are being used in the current study and details are presented in Table 1. Cloud obstructs the AOD observation in pre-monsoon and monsoon seasons particularly in DBR when observation was possible only for 60 days whereas the no of days of observation in that season are between 157 in IPH and 206 in AGA. In monsoon number of days of observation varies between 74 in DBR and 256 in AGA while the same are within 92 in SHN and 144 in AGA in ret-monsoon. While the MTOP was periodically calibrated at the factory, the MWR was inter compared with the MTOPs for consistency.

From the spectral AOD, the Ångström wavelength exponent α, has been derived over entire wavelength regime, through the Ångström's formula

$$\tau_\lambda = \beta\lambda^{-\alpha} \tag{1}$$

where τ_λ is AOD at wavelength λ (in μm) and β is the optical depth at $\lambda = 1$ μm related to aerosol loading in the column. $\alpha \leq 1$ indicates size distributions dominated by coarse mode aerosols (radii >0.5 μm) and $\alpha \geq 1$ by fine mode aerosols (radii <0.5 μm).

2.3.2. Vertical distribution of aerosols

The Cloud-Aerosol Lidar and Infrared Pathfinder Satellite Observations (CALIPSO) provides a global, multi-year data set of cloud and aerosol spatial and optical properties (Winker et al., 2007 and references therein). The extinction coefficient at 532 nm with 5 m vertical resolution retrieved by CALIPSO over the NER (https://eosweb.larc.nasa.gov) are utilised in order to examine the altitude profiles of extinction due to aerosols. The bin averaged (3 bins) daily (both day and night) extinction profiles are grouped seasonally for all the four locations for the period October 2010–December 2013.

2.3.3. Identification of distant source region

The HYSPLIT (Hybrid Single-Particle Lagrangian Integrated Trajectory) model of National Atmospheric and Oceanic Administration (NOAA) has been used to calculate the isentropic back trajectories to understand the possible flow paths of airmass that would help to identify the source regions. This model uses the Ward's hierarchical method (Ward, 1963) to form clusters by combining the nearest trajectories in order to delineate the distinct mean pathways of the trajectories. The seasonal mean airmass back trajectories arriving at the four stations: DBR, IPH, SHN and AGA at altitudes 0.5 km, 1.5 km and 3.5 km are analyzed in this study.

2.3.4. Estimation of aerosol radiative forcing (ARF) and atmospheric heating rate

In order to estimate the ARF the widely used Santa Barbara DISORT Atmospheric Radiative Transfer model (Ricchiazzi et al., 1998) has been deployed. The necessary optical parameters required by the SBDART are obtained from the Optical Properties of Aerosols and Clouds (OPAC) (Hess et al., 1998) model for user defined aerosol mixture. Based on the AOD and BC values observed in the respective locations 'continental average' aerosol model in OPAC is considered for DBR and IPH and 'continental polluted' for AGA and SHN following d'Almeida et al. (1991). The number density of each component in the aerosol mixture (composed of water soluble, insoluble, soot, mineral transported, sulphate, sea salt coarse/accumulation aerosols) is adjusted to fit the measured AOD spectra within 5% error, keeping black carbon aerosol number density/fraction measured using an Aethalometer as an anchoring point. This is a widely used method and detail methodology is available elsewhere (Satheesh et al., 2010; Pathak et al., 2010 and references therein). Aerosol spectral optical depths in the entire shortwave region as well as the spectral values of single scattering albedo (SSA) and asymmetry parameter (g) are used as inputs in SBDART to simulate solar irradiance for different solar zenith angles, which are further used to calculate the diurnally averaged aerosol radiative forcing at Top of the Atmosphere (TOA) and at the surface (SUR). The difference between the ARF at the TOA and SUR gives the atmospheric forcing, later being the representative of heating of the atmosphere due to the presence of aerosols. The heating rate of the atmosphere is estimated following the equation

$$\frac{\partial T}{\partial t} = \frac{g}{C_p}\frac{\Delta F_A}{\Delta P} \tag{2}$$

where $\partial T/\partial t$ is the heating rate (K day^{-1}), g is the acceleration due to gravity, C_P (1006 J kg^{-1} K^{-1}) is the specific heat capacity of air at constant pressure, ΔP (=300 hPa) is the change in the atmospheric pressure, and F_A is the estimated atmospheric forcing.

3. Results and discussion

3.1. Aerosol distribution in NER: regional characterization

The tropical and subtropical climatic conditions coupled with complex topography introduce strong temporal and spatial het-

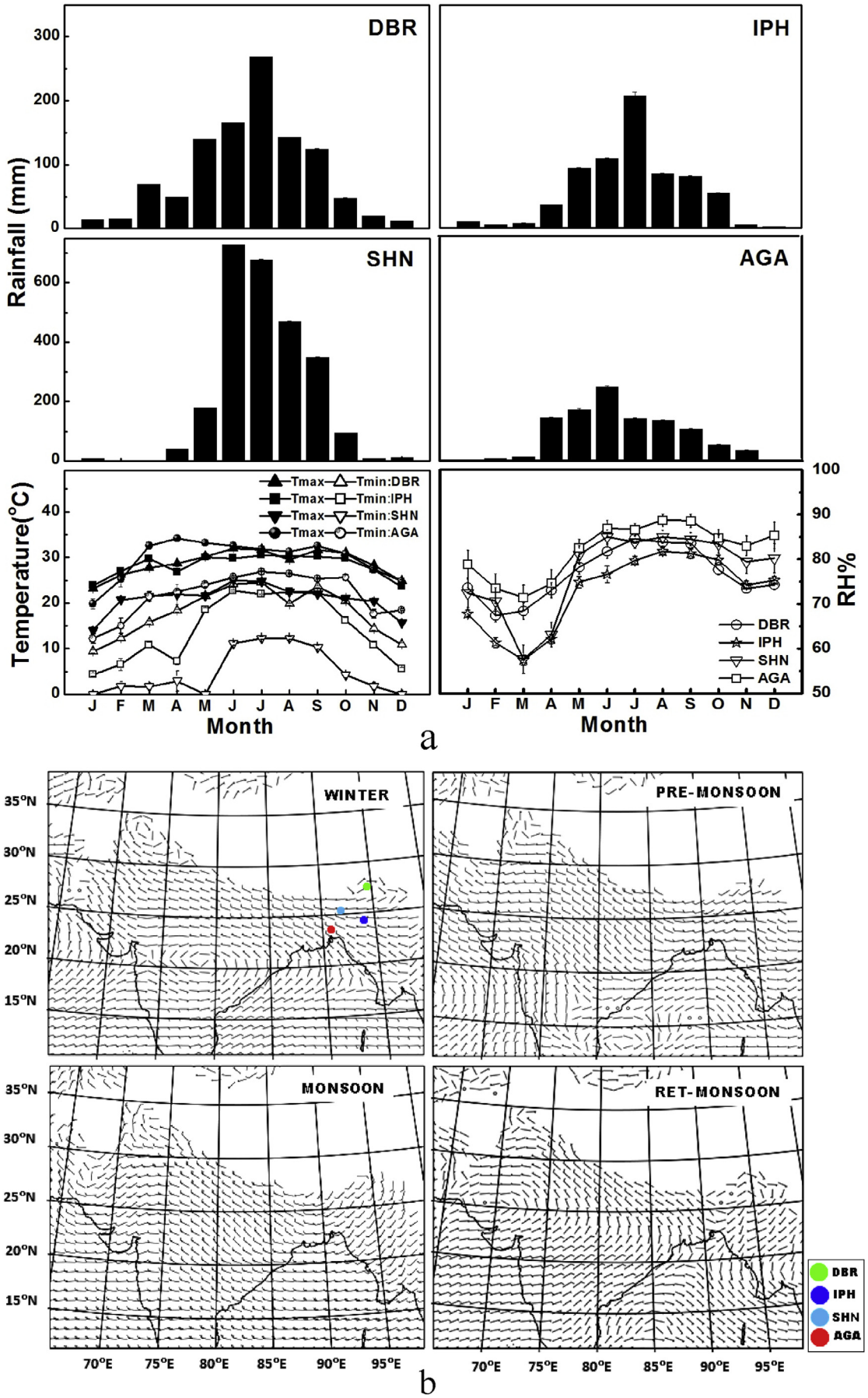

Fig. 2. (a). Annual variation of total rainfall (top 4 panels), Maximum (T_{Max}) and Minimum (T_{min}) temperatures (bottom left panel) and Relative Humidity (RH) for the four stations: Dibrugarh (DBR), Imphal (IPH), Shillong (SHN) and Agartala (AGA). The vertical bars in Temperature and RH represent one standard deviation from the mean. (b). Synoptic wind patterns at 850 hPa level generated using WRF-Meteorology for Indian subcontinent and adjoining regions for seasons: winter, pre-monsoon, monsoon and retreating monsoon. The dots represents the study locations.

Table 1
Details of the study locations, Instrumentation, Seasonal and climatological mean AOD (Aerosol Optical Depth) measured with Multi Wavelength Radiometer (MWR) and Microtops (MTOP) at Dibrugarh (DBR), Imphal (IPH), Shillong (SHN), Agartala (AGA) for the four seasons Winter (W), Pre-monsoon (PM), Monsoon (M) and Retreating monsoon (RM). The numbers within the parenthesis indicate number of days of observations.

Station	Geographical details			Instrumentation & seasonal AOD					Climatological AOD
	Lat (°N)	Long (°E)	Alt (m asl)	Instrument	W	PM	M	RM	
DBR	27.3	94.6	111	MWR	0.51 (24)	0.64 (60)	0.28 (74)	0.23 (94)	0.41 (352)
IPH	24.75	93.92	765	MTOP	0.38 (192)	0.59 (157)	0.32 (134)	0.29 (124)	0.40 (607)
SHN	25.6	91.9	1496	MWR/MTOP	0.53 (159)	0.74 (159)	0.41 (104)	0.38 (92)	0.52 (514)
AGA	23.9	91.2	14.9	MTOP	0.74 (216)	0.80 (206)	0.54 (256)	0.58 (144)	0.67 (822)

erogeneity in aerosol characteristics over the south Asian region. The AOD over the NER shows spatial variability from east to west (Fig. 3). The dots in the figure whose sizes are function of AOD values indicate the climatological AOD averaged for the study period mentioned above. The aerosol loading is found to be the highest in the westernmost location AGA ($\tau_p = 0.67 \pm 0.20$) and lowest in the eastern location IPH ($\tau_p = 0.40 \pm 0.14$). The station SHN, despite being at a much higher elevation than the other three, exhibits the second highest AOD value. Appreciable climatological mean AODs are observed at all the stations, notwithstanding the low population density (except AGA) and the highly vegetated environment of the NER. This can be explained based on the fact that, the study locations being the capital cities of different states (except DBR) are urban pockets within the usual rural environment of NER. It is well known again that the rural areas are associated with large aerosol sources due to fuel consumption, including biofuels used for domestic purposes. Babu et al. (2013) have reported high increasing rate of aerosol loading in rural areas compared to urban locations in India. Thus the local pollution such as emissions from brick kilns, oil/gas fields and coal mines and other anthropogenically generated aerosols from biofuel/fossil fuel emissions are major sources of aerosols in the region. Estimates as on 2013 depicts that the state of Assam in NER is having ~59% registered vehicles followed by Manipur (IPH) with 7.7%, Tripura (AGA) with 7% and Meghalaya (SHN) with 6.4%, which are highly concentrated in the urban centres. IPH is influenced by urban pollution while AGA is heavily influenced by soil dust. Again, the western locations AGA and SHN, being located at the outflow pathways of winter haze from IGP, exhibit appreciable aerosol loading in winter. On the other hand the other two stations DBR and IPH are comparatively less affected by winter haze. Moreover, the high AOD in AGA may be attributed to the fact that being close to Bangladesh, the site is exposed to the influence of the heavy pollution in the plains of Bangladesh. On the other hand, open coal mines are predominant in SHN which adds to the urban pollution there. There are number of cement factories, emissions from which in addition to that from the Shillong city may be trapped in the valley where the measurements are made. DBR is a growing city in terms of industrialization and urbanization while IPH is an urban pocket in the eastern part of the NER, thus both showing appreciable aerosol loading. Another major source of natural aerosols in this region is the secondary aerosols produced by the biogenic volatile organic compounds (BVOCs) emitted by natural forests. In NER 66% of total area is covered by forest and thus primary biological aerosols are also abundant.

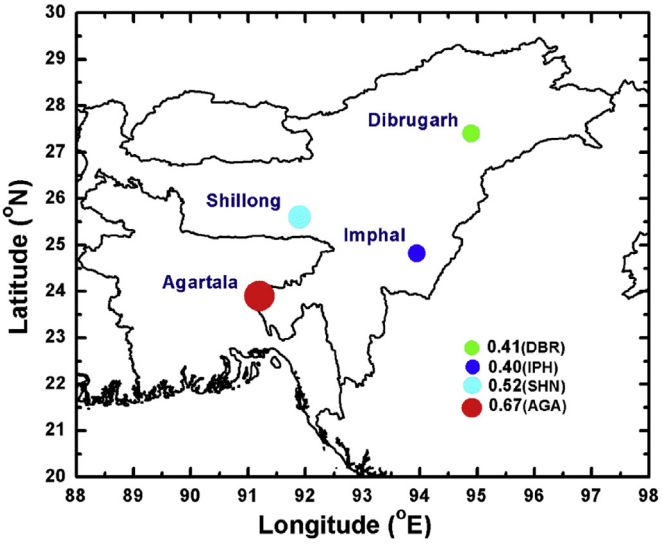

Fig. 3. Spatial variability of climatological average AODs over NER. The bubble size is a function of the magnitude of AOD of the respective locations.

As seen in Fig. 4(a) AOD in DBR, IPH and SHN exhibit an annual variation with the peak value in the pre-monsoon season, particularly in the month of March. In AGA on the other hand AOD remains at a nearly equal level from January to May after which it follows the trend as at the other stations i.e., a monsoon minimum and a slow buildup in the retreating monsoon season. Similar seasonal AOD cycle with pre-monsoon peak and retreating monsoon dip in AOD has been reported from Dibrugarh by Bhuyan et al. (2005), Gogoi et al. (2009) and Pathak et al. (2010). Heavy monsoon rains effectively remove soluble gases and aerosol, which results in lowering of aerosol load in that season. The lowest AOD observed in retreating monsoon season is the representative of the background aerosol condition (Pathak et al., 2012) and is assigned to the combined effect of local meteorological conditions and topography of the region (Gogoi et al., 2011). In winter under favourable meteorological conditions like scanty rainfall resulting in longer residence time of aerosols in the atmosphere leads to appreciable aerosol burden.

The western location AGA exhibit significant aerosol loading (AOD > 0.6) in the winter and pre-monsoon season. On the other hand, in DBR, IPH and SHN, AOD > 0.6 is observed only in the pre-monsoon season. The day to day AOD variability is high during November–May at all the locations, when various type of outdoor burning activities occur (Pathak et al., 2010). In Fig. 4(b) the frequency of occurrence of AOD within each bin (in steps of 0.2) ranges are shown for the four stations. In DBR, on 30–35% of days AOD remains within 0.2–0.4, AOD > 0.4 occurs on less than 20% the days of observation. Percentage occurrence of high AOD > 0.6 is low and AOD > 1.0 are rarely measured. In IPH on >40% of the days AOD remains around 0.4, it is in the range 0.6–0.8 on ~25% of the days while AOD > 0.8 or more is infrequent. Similarly, in SHN also the frequency of occurrence is high for low AOD which decreases progressively for higher AOD values. In contrast frequency distribution is different for AGA. Each of AOD values 0.4, 0.8 and 1.0 occurs on nearly 20% of the days while high AOD > 1.2 occurs on 10% of the days.

Pathak et al. (2010, 2012) have attributed biomass burning and transported aerosols along with the other local sources as the

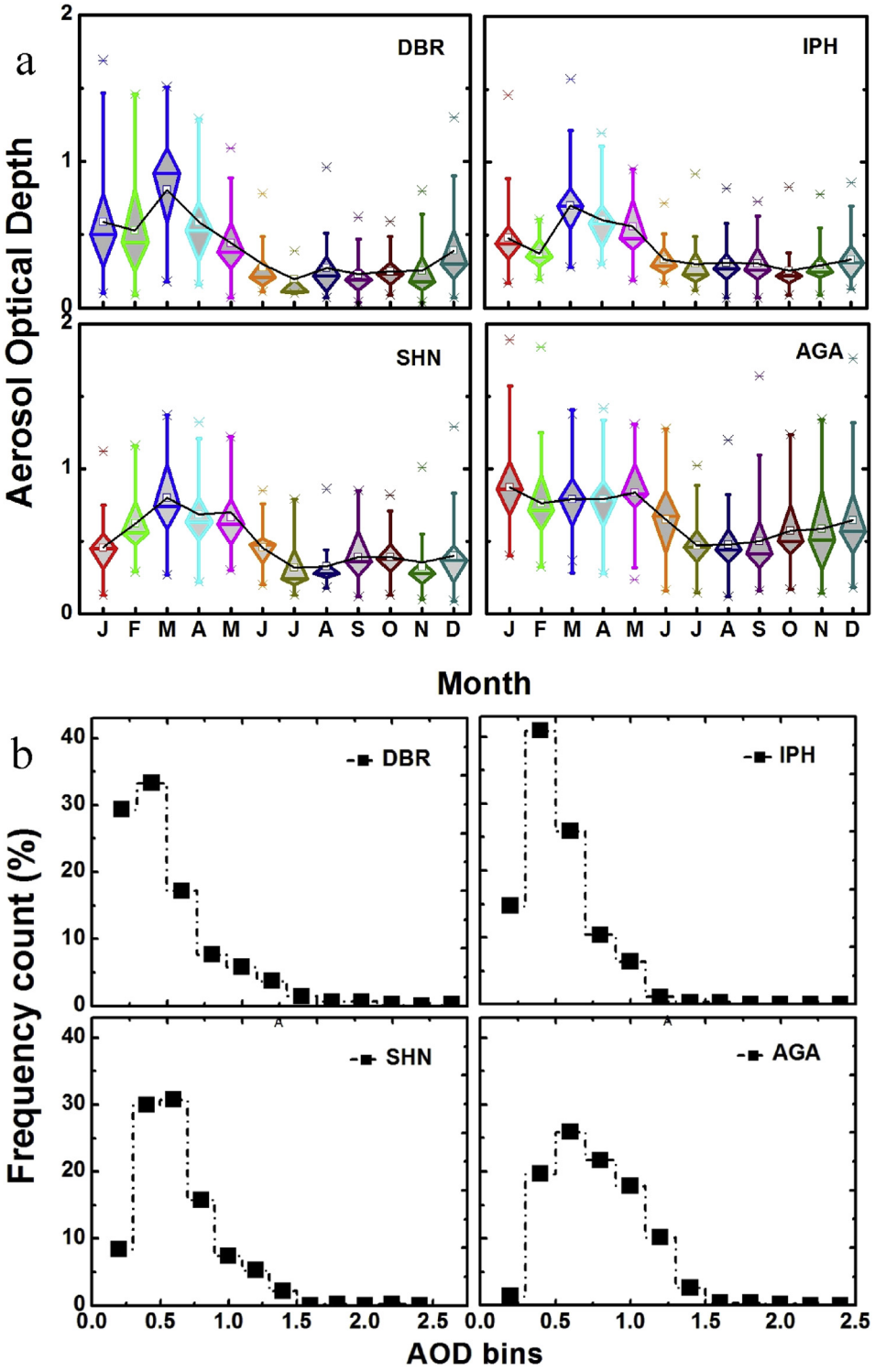

Fig. 4. (a). Box plot showing month to month variation of mean AOD at the four stations. The vertical lines represent the standard deviation from the mean. Each box represents 25th and 75th percentiles and the whiskers represent the 5th and 95th percentiles. The small box inside each box represents the mean value and the horizontal line represents the median value. (b). Frequency of occurrence of AOD at the four locations in NER: Dibrugarh (DBR), Imphal (IPH), Shillong (SHN) and Agartala (AGA).

contributor of seasonal aerosol burden particularly in the pre-monsoon and winter seasons in Dibrugarh, NER. These have been re-discussed here in order to evaluate the regional picture of the aerosol loading. The severe anthropogenic biomass burning experienced in NER, particularly in pre-monsoon is illustrated in Fig. 5. Table 2 also shows the number of fire counts averaged for different regions of south, east and south-east Asia. The number of fire counts in NER particularly in pre-monsoon (198) exceeds any other region of the Asia. But in winter east and south-east Asia exceeds in fire count number. It is worthwhile to mention here that the anthropogenic biomass burning associated with shifting cultivation in NER and other regions of South Asia causes the observed

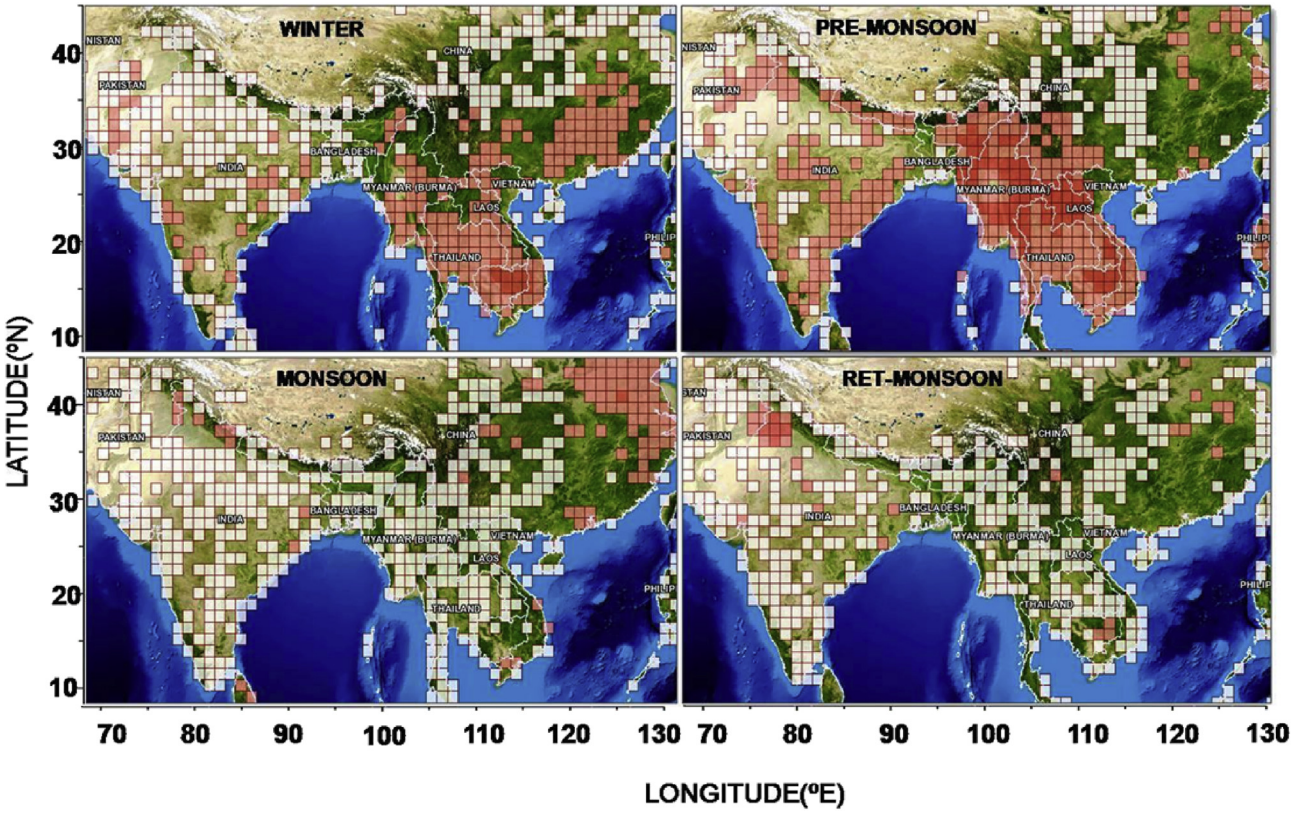

Fig. 5. Seasonal MODIS retrieved fire count map covering South, South-East and East Asia.

fire activities while natural forest fire is predominant in south-east Asia. The prevailing westerly winds, combined with the orography of the IGP that spatially confines the aerosols into a rather narrow channel and leads to the outflow into the northern and head Bay of Bengal (BoB), results in the large loading of aerosols in that region (Girolamo et al., 2004; Nair et al., 2007; Niranjan et al., 2007). The eastern coastal belt of India, comprising several ports and industries, is a hot spot of accumulation mode aerosols (e.g., Moorthy et al., 2005). This is indicated by the very high values observed over Visakhapatnam and Bhubaneswar during Winter ICARB (Moorthy et al., 2010 and references therein). These regions are found to influence the aerosol environment in NER in all seasons. Eleven distinct advection pathways namely IGP, southern India, northern Arabian Sea and west Asian desert region, southern Arabian Sea, East coast of India, Myanmar and East Asia have been identified on the basis of trajectory clustering (Fig. 6 and Table 3). The influence of the pollution in Bangladesh in AGA is revealed by the back trajectories which reach AGA always traversing Bangladesh. In monsoon 5 days back trajectories reaching at all the locations except DBR originate at Arabian Sea carrying sea salt particles. It is well established that Arabian Sea is characterized by loading due to natural aerosols (e.g., dust and sea salt) and the BoB by anthropogenic aerosols. Thus unlike other locations trajectories from BoB carries moisture and pollutants towards DBR. Thus external influence significantly determines the aerosol environment in the region.

Table 2
Fire count numbers detected by MODIS-Aqua satellite averaged for October 2010–September 2014 for different regions of Indian Subcontinent including NER and Asia for the four seasons Winter (W), Pre-monsoon (PM), Monsoon (M) and Retreating monsoon (RM).

Regions	PM	M	RM	W
NER (22–30°N, 88–98°E)	198	4	3	27
IGP (19–30°N, 76–88°E)	38	7	16	9
South India (8–19°N, 72–94°E)	28	12	6	14
West India (19–30°N, 68–76°E)	14	4	32	9
Central India (19–25°N, 76–84°E)	49	6	6	11
East and south-east Asia (10–45°N, 98–140°E)	58	12	10	42

3.2. Particle size distribution

The annual variation of Angstrom exponent α (indicator of the aerosol size distribution) is presented in Fig. 7 which exhibits consistent spatio-temporal variation. It is lowest in the monsoon months of July/August due to drastic decrease in the influence of sub-micron aerosols during the rainy period associated with wet removal processes. On the other hand it attains annual peak in winter with the production of submicron aerosols mostly from anthropogenic activities discussed in the previous section along with the indoor/outdoor burning in cold season. Spatially, the westernmost station SHN depicts the lowest values of α in any month, notwithstanding that the station is at much higher elevation (~1.4 km above mean sea level) than the other three stations. This may be associated with the emission of coarse aerosols from the open coal mines situated near the study location and urban dust from upwind Shillong city. The highest value for the exponent occurs at the eastern most station DBR followed by IPH. Hence these two stations are characterized by fine aerosols whereas SHN and AGA are rich in coarse mode aerosols originating from soil dust in dry months, particle aging under hazy condition (particularly in winter). Thus there is a distinct east-west asymmetry in aerosol distribution within the NER with higher aerosol loading in western locations AGA and SHN.

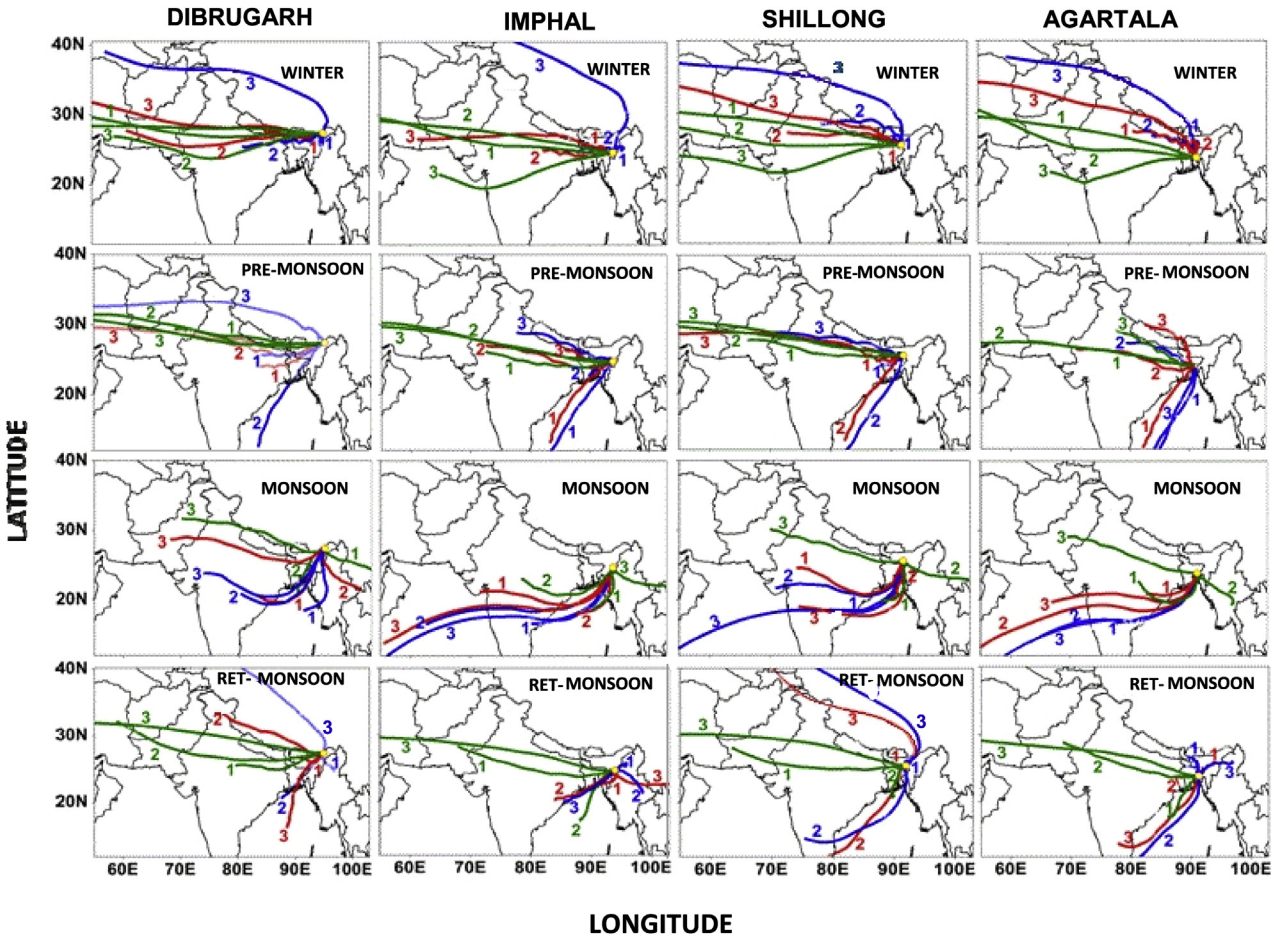

Fig. 6. Back trajectories at different seasons: Pre-monsoon, monsoon, ret-monsoon and winter arriving at the four locations in NER: Dibrugarh, Imphal, Shillong and Agartala at altitudes 500 m AGL, 1500 m AGL and 3500 m AGL.

3.3. Aerosol characteristics in Asia: regional distribution

The seasonal mean values of AOD and α, as reported by different investigators over the Asian countries, have been compared in order to identify the similarities or otherwise with other regions of Asia in respect of aerosols (Supplementary table). On an average the NER region behaves similar to most of the regions/locations in Asia with pre-monsoon high AODs (except West India, where AOD reaches its peak level in monsoon). NER behaves like the East/South-East/West Asia and the Himalayan region with minimal aerosol burden in the retreating monsoon, while the IGP, south India and the oceanic region show lowest AOD in monsoon. In mon-

Table 3
Seasonal percentage trajectories in each cluster arriving at three altitudes 0.5 km, 1.5 km and 3.5 km above ground level (AGL) in the four locations Dibrugarh, Imphal, Shillong and Agartala during different seasons.

Trajectory ratio (%)													
Seasons		Winter			Pre-monsoon			Monsoon			Retreating monsoon		
Station	Cluster no	Altitude											
		0.5 km AGL	1.5 km AGL	3.5 km AGL	0.5 km AGL	1.5 km AGL	3.5 km AGL	0.5 km AGL	1.5 km AGL	3.5 km AGL	0.5 km AGL	1.5 km AGL	3.5 km AGL
Dibrugarh	1	76	56	67	74	41	44	35	56	41	52	60	42
	2	16	34	20	20	40	39	34	37	37	34	23	32
	3	8	10	13	6	19	17	31	7	22	14	17	26
Imphal	1	83	61	42	37	38	49	41	58	38	56	57	41
	2	16	25	32	36	37	34	33	33	36	30	35	37
	3	1	14	26	27	25	17	26	9	26	14	8	22
Shillong	1	71	49	36	41	57	54	40	44	64	89	86	57
	2	18	33	33	31	30	41	39	30	24	6	11	26
	3	11	18	31	28	13	5	21	26	12	5	3	17
Agartala	1	47	53	41	50	53	54	39	53	54	77	46	42
	2	41	40	34	41	30	26	37	35	38	15	44	33
	3	12	7	25	9	17	20	24	12	8	8	10	25

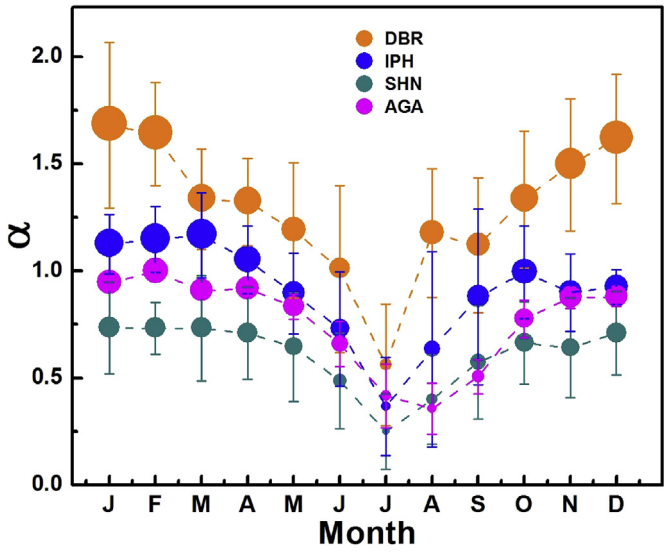

Fig. 7. Time series plot of Ångström Exponent, α at the four locations in NER: Dibrugarh (DBR), Imphal (IPH), Shillong (SHN) and Agartala (AGA). The bubble sizes are the function of the values of α. The vertical lines represent one standard deviation from the mean.

soon, NER AOD is comparable to East and South-East Asian AOD, exceeding that in the Himalayan region and South India but lower than the IGP and west Asia. Unlike NER and other regions in IGP, AOD maximizes during retreating monsoon. This establishes regional variability in aerosol loading, which is strongly related to sources. Climatologically, NER ranks second highest in aerosol loading with regional average AOD of 0.49 ± 0.2 next to IGP region (0.64 ± 0.2) followed by East/South-East Asia and South India.

The NER is dominated by fine mode aerosols ($\alpha \geq 1$) in general like the east and south-east Asia and IGP (Supplementary table). The aerosol column is dominated by coarse mode particles ($\alpha \leq 1$) in pre-monsoon in East Asia while for NER, south India and IGP coarse particles are predominant in monsoon. The α value ≤ 1 in West India and Himalaya and Tibetan plateau region during pre-monsoon and monsoon season indicates size distributions dominated by coarse aerosols mostly associated with dust or sea salt.

3.4. Vertical distribution of aerosols in NER

The spatio-temporal distribution of vertical extinction profiles at 532 nm as obtained from CALIPSO Lidar measurements over each location is illustrated seasonally in Fig. 8. The profiles were selected for satellite passes with 1° × 1° grid cantered around each location. The extinction is found to be highest in AGA followed by SHN particularly within 2 km. This is corroborated with the maximum AOD observed in AGA and that followed by SHN. In general distinct elevated aerosol layers are present between 2 and 4 km in all the stations during most of the seasons. But in IPH the elevated layers are observed from 1 to 3 km in winter. Interestingly, during the main summer monsoon period (July and August) the possibility of transport of air masses from central India to the BoB, then northwards over Bangladesh and up into the Himalayas is evident (Lawrence and Lelieveld, 2010) across the NER under the influence of Tibetan Plateau anticyclone. The ret-monsoon season being affected by monsoon wet scavenging possesses there is a less

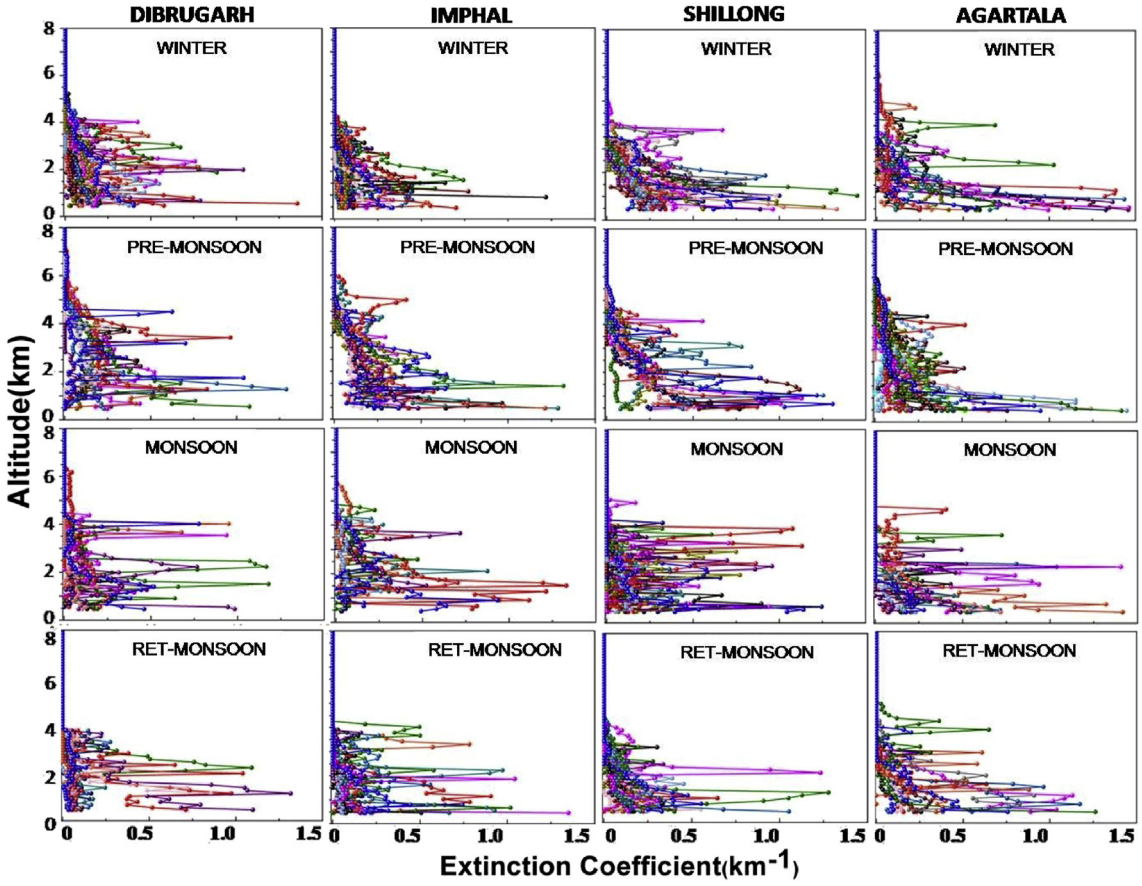

Fig. 8. Seasonal distribution of CALIPSO derived vertical profiles of extinction co-efficient at 532 nm at the four locations in NER: Dibrugarh, Imphal, Shillong and Agartala. The seasons: Winter, Pre-monsoon, Monsoon, Ret-monsoon are arranged serially from top to bottom.

probability of aerosol build up at elevated altitudes. However, few profiles with signature of elevated aerosols during this season are also prominent. Scanty rain along with long range transportation in winter results in accumulation of aerosols at higher altitudes in addition to that near the surface (Gogoi et al., 2011). The trajectories above the boundary layer (1.5 km and 3.5 km) discussed in previous section are attributed to the observed elevated aerosol layers over NER. Several studies across the Indian subcontinent show the elevated aerosol layers at an altitude of ~2–4 km above the local boundary layer formed due to the long-range transport of aerosols from distant locations (Ramana et al., 2004; Niranjan et al., 2007; Gautam et al., 2010; Mishra et al., 2010). Ramana et al. (2004) reported elevated aerosol layers in northern India, particularly during the winter season which they have attributed to dry convective lifting of pollutants from distant sources and subsequent horizontal upper air long range transport. Mishra et al. (2010) from micro pulse Light Detection and Ranging (LIDAR) observed a mineral dust layer at the west coast of peninsular India which according to them is due to advection of air mass from arid regions around western Arabian Sea. LIDAR observation by Satheesh et al. (2008) showed that during pre-monsoon, most of Indian region is characterized by elevated absorbing aerosol layers up to 4 km over central India. In the north eastern region also aerosol layers within 3–5 km has earlier been reported by Sharma et al. (2009) from satellite observation.

3.5. Climatic implications of aerosols

The climatic implication of aerosols is represented in terms of the aerosol radiative forcing (ARF). The ARF in the atmosphere gives the amount of radiation flux absorbed by the atmosphere due to presence of aerosols. This energy gets converted into heat thereby resulting in heating of the atmosphere. The direct ARF may contribute to the weakening of the Asian monsoon system (Li et al., 2007 and references therein). In Fig. 9 the seasonal ARF at top of the atmosphere (TOA), at the surface (SUR) and the in the atmosphere (ATM) estimated using the method described in the four locations are presented. The TOA ARF estimated during the study period over the NER locations varies from −9.4 Wm^{-2} in IPH in pre-monsoon to 0.94 Wm^{-2} in SHN in retreating monsoon season (Fig. 9). The positive or less negative TOA ARF particularly in retreating monsoon and winter seasons is associated with higher BC fraction over all the locations. Further, the absorbing aerosols above the low level clouds which explain about 20% of the global burden but 50% of the forcing (Zarzycki and Bond, 2010) may have an influence on the enhanced (less negative) TOA forcing over this region. The low-level cloud can reflect solar radiation effectively and so absorbing aerosols above low cloud have more absorption (Podgorny and Ramanathan, 2001). Previously, Pathak et al. (2010) have reported the less negative TOA forcing over DBR. The highest surface ARF, which is associated with surface dimming, occurs in the pre-monsoon season ranging from −34.5 Wm^{-2} in DBR to −53.8 Wm^{-2} SHN followed by winter. On the other hand, in AGA maximum surface forcing is observed in winter (−56.5 Wm^{-2}) and is followed by pre-monsoon season. At the expense of this surface forcing (or cooling) atmosphere in AGA in winter is warmed by 56.2 Wm^{-2} or 1.6 K day^{-1}. On the other hand, highest atmospheric forcing occurs in the pre-monsoon season ranging from 31.6 Wm^{-2} in SHN to 25.1 Wm^{-2} in IPH. The heating of the atmosphere due to aerosols is found to occur in the other locations IPH, DBR and SHN in the pre-monsoon season by 0.7 K day^{-1}, 1.0 K day^{-1} and 1.2 K day^{-1} respectively. In the locations AGA and SHN observed higher forcing values are associated with high AODs compared to the other two locations. Also BC concentrations (not reported here), exhibiting similar spatial variation in NER determines the forcing as well as heating in the atmosphere. However, in ret-monsoon surface forcing as well as atmospheric heating is comparatively small due to less abundance of aerosols. Earlier Pathak et al. (2010) have also shown the resemblance between the seasonal ARF with the AOD values in DBR. Apart from AOD and BC fraction, the ARF is also a function of other optical and physical parameters like SSA, g, α, vertical extinction coefficient, black carbon fraction, aerosol particle size as well as surface reflectance etc. The ATM ARF in AGA is found to be greater than estimations over Trivandrum, Ahmedabad and Visakhapatnam (Pathak et al., 2010 and references therein). Seasonal highest forcing in general over Indian subcontinent exhibit spatio-temporal variability, for example, in Trivandrum it is in winter like AGA, but in Visakhapatnam and Ahmedabad seasonal highest ATM ARF is reported in retreating (post) monsoon and monsoon seasons respectively (Pathak et al., 2010 and references therein).

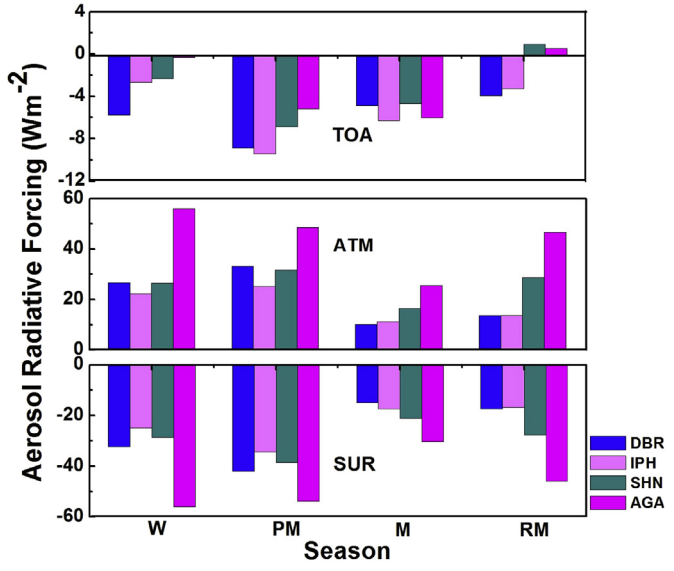

Fig. 9. Aerosol radiative forcing at Top of the Atmosphere (TOA), at the surface (SUR) and in the atmosphere (ATM) over the four locations in NER: Dibrugarh (DBR), Imphal (IPH), Shillong (SHN) and Agartala (AGA) during pre-monsoon (PM), monsoon (M), retreating monsoon (RM) and winter (W) for the period October 2010–September 2014.

As the NER behaves as a sink region for the aerosols, the heavy aerosol loading at different altitudes may sustain for longer period of time thereby heating the atmosphere as well as can contribute to frequent cloud formation under the influence of advocated moisture from BoB. Thus aerosols in this region play a crucial role in both direct and indirect effect of aerosols, on atmospheric circulation and hence monsoon, which needs further investigation. Also, the impact of aerosols on extreme weather conditions particularly in monsoon season and on the decreasing precipitation trend in the NER are auxiliary issues to be explored. Present study is expected to help in these regards.

4. Conclusions

Spatio-temporal distribution of aerosols and its implications are studied in North-Eastern Region of India based on a long term ARFINET database. Following conclusions are drawn from the study.

- Aerosol burden in the NER like most of the locations in South and South-East Asia exhibit maximum values in pre-monsoon season. But unlike many locations, this region exhibit lowest aerosol loading in retreating monsoon season.
- Aerosol optical depth exhibits an east-west asymmetry within the NER with higher values in the western locations Agartala

and Shillong compared to the eastern locations Dibrugarh and Imphal. The western locations are influenced by both natural aerosols (sea salt and soil dust) and anthropogenic aerosols produced locally or transported from Indo Gangetic plains and Bangladesh.

- NER ranks second highest in aerosol loading in the Asian region with regional average AOD ~ 0.49 next to the IGP region (AOD ~ 0.64) followed by East/South East Asia and south India.
- Elevated aerosol layers in the region form mostly due to upper air transportation.
- Strong surface forcing due to the presence of aerosols is experienced in NER with surface aerosol radiative forcing of ~ −56.5 Wm^{-2} and heating of 1.6 K day^{-1}, which exceeds or are comparable to those in many of the locations especially in the Indian subcontinent.

Acknowledgements

Authors are thankful to the Indian Space Research Organisation (ISRO) for financial support under its GBP ARFI Project and CALIPSO, MODIS & ARL Science team for scientific database. We thank the anonymous reviewers for their helpful comments and suggestions towards improvement of the paper.

Appendix A. Supplementary data

Supplementary data related to this article can be found at http://dx.doi.org/10.1016/j.atmosenv.2015.07.038.

References

Adak, A., Chatterjee, A., Kumar, S.A., Sarkar, C., Ghosh, S., Raha, Si, 2014. Atmospheric fine mode particulates at Eastern Himalaya, India: role of meteorology, long-range transport and local anthropogenic sources. Aerosol Air Qual. Res. 14, 440–450.

Babu, S.S., Moorthy, K.K., Manchanda, R.K., Sinha, P.R., Satheesh, S.K., Vajja, D.P., Srinivasan, S., Arun Kumar, V.H., 2011. Free tropospheric black carbon aerosol measurements using high altitude balloon: do BC layers build "their own homes" up in the atmosphere? Geophys. Res. Lett. L08803. http://dx.doi.org/10.1029/2011GL046654.

Babu, S.S., Manoj, M.R., Moorthy, K.K., Gogoi, M.M., Nair, V.S., Kompalli, S.K., Satheesh, S.K., Niranjan, K., Ramagopal, K., Bhuyan, P.K., Singh, D., 2013. Trends in aerosol optical depth over Indian region: potential causes and impact indicators. J. Geophys. Res. Atmos. 118, 11,794–11,806. http://dx.doi.org/10.1002/2013JD020507.

Bonasoni, P., Laj, P., Marinoni, A., Sprenger, M., Angelini, F., Arduini, J., Bonafè, U., Calzolari, F., Colombo, T., Decesari, S., Di Biagio, C., di Sarra, A.G., Evangelisti, F., Duchi, R., Facchini, M.C., Fuzzi, S., Gobbi, G.P., Maione, M., Panday, A., Roccato, F., Sellegri, K., Venzac, H., Verza, G.P., Villani, P., Vuillermoz, E., Cristofanelli, P., 2010. Atmospheric brown clouds in the Himalayas: first two years of continuous observations at the Nepal climate observatory-pyramid (5079 m). Atmos. Chem. Phys. 10, 7515–7531.

Bhuyan, P.K., Gogoi, M.M., Moorthy, K.K., 2005. Spectral and temporal characteristics of aerosol optical depth over a wet tropical location in North East India. Adv. Space Res. 35, 1423–1429.

Cao, J., Tie, X., Xu, B., Zhao, Z., Zhu, C., Li, G., Liu, S., 2010. Measuring and modeling black carbon (BC) contamination in the SE Tibetan Plateau. J. Atmos. Chem. 67, 45–60.

Chin, M., Rood, R.B., Lin, S.J., Muller, J.F., Thompson, A.M., 2000. Atmospheric sulfur cycle simulated in the global model GOCART: model description and global properties. J. Geophys. Res. 105, 24 671–24 687.

d'Almeida, G.A., Koepke, P., Shettle, E.P., 1991. Atmospheric Aerosols-global Climatology and Radiative Characteristics. A. Deepak, Hampton, VA.

Dumka, U.C., Moorthy, K.K., Tripathi, S.N., Hegde, P., Sagar, R., 2011. Altitude variation of aerosol properties over the Himalayan range inferred from spatial measurements. J. Atmos. Sol. Terr. Phys. 73, 1747–1761.

Gautam, R., Hsu, N.C., Lau, K.M., 2010. Premonsoon aerosol characterization and radiative effects over the Indo Gangetic Plains: implications for regional climate warming. J. Geophys. Res. 115, D17208. http://dx.doi.org/10.1029/2010JD013819.

Gogoi, M.M., Moorthy, K.K., Babu, S.S., Bhuyan, P.K., 2009. Climatology of columnar aerosol properties and the influence of synoptic conditions: first time results from the northeastern region of India. J. Geophys. Res. 114, D08202. http://dx.doi.org/10.1029/2008JD010765.

Gogoi, M.M., Pathak, B., Moorthy, K.K., Bhuyan, P.K., Babu, S.S., Bhuyan, K., Kalita, K., 2011. Multi-year investigations of near surface and columnar aerosols over Dibrugarh, northeastern location of India: heterogeneity in source impacts. Atmos. Environ. 45, 1714–1724.

Gogoi, M.M., Moorthy, K.K., Kumar, K.S., Chaubey, J.P., Babu, S.S., Manoj, M.R., Nair, V.S., Prabhu, T.P., 2014. Physical and optical properties of aerosols in a free Tropospheric environment: results from long-term observations over western trans-Himalayas. Atmos. Environ. 84, 262–274.

Girolamo, L.D., Bond, T.C., Bramer, D., Diner, D.J., Fettinger, F., Kahn, R.A., Martonchik, J.V., Ramana, M.V., Ramanathan, V., Rasch, P.J., 2004. Analysis of Multi-angle Imaging Spectroradiometer (MISR) aerosol optical depths over greater India during winter 2001–2004. Geophys. Res. Lett. 31, L23115. http://dx.doi.org/10.1029/2004GL021273.

Guha, A., De, B.K., Dhar, P., Banik, T., Chakraborty, M., Roy, R., Choudhury, A., Gogoi, M.M., Babu, S.S., Moorthy, K.K., 2015. Seasonal characteristics of aerosol black carbon in relation to long range transport over Tripura in northeast India. Aerosol Air Qual. Res. 15, 786–798. http://dx.doi.org/10.4209/aaqr.2014.02.0029.

Hess, M., Koepke, P., Schultz, I., 1998. Optical properties of aerosols and clouds: the software package OPAC. Bull. Am. Meteorol. Soc. 79, 831–844.

Holben, B.N., Eck, T.F., Skitsker, I., Tanré, D., Bziis, J.P., Setzer, A., Vermote, E., Reagan, J.A., Kazlfnzan, Y.J., Nnknjima, T., Lauemi, F., Jankozoink, I., Smimov, A., 1998. AERONET—a federated instrument network and data archive for aerosol characterization. Remote Sens. Environ. 66, 1–16.

Khare, P., Baruah, B.P., 2010. Elemental characterization and source identification of $PM_{2.5}$ using multivariate analysis at the suburban site of North-East India. Atmos. Res. 98, 148–162.

Krinner, G., Boucher, O., Balkanski, Y., 2006. Ice-free glacial northern Asia due to dust deposition on snow. Clim. Dyn. 27, 613–625.

Kompalli, S.K., Babu, S.S., Moorthy, K.K., Gogoi, M.M., Nair, V.S., Chaubey, J.P., 2014. The formation and growth of ultrafine particles in two contrasting environments: a case study. Ann. Geophys. 32, 817–830.

Lawrence, M.G., Lelieveld, J., 2010. Atmospheric pollutant outflow from southern Asia: a review. Atmos. Chem. Phys. 10, 11017–11096.

Liu, J., Mauzerall, D.L., Horowitz, L.W., 2009. Evaluating inter-continental transport of fine aerosols: (2) global health impact. Atmos. Environ. 43, 4339–4347.

Li, X., Zou, X., Zhu, X., Zhang, M., Zhu, Y., Zhou, S., Jin, F., Cai, M., 2004. Observation, Theory and Modeling of Atmospheric Variability: Selected Papers of Nanjing Institute of Meteorology Alumni in Commemoration of Professor Jijia Zhang. In: World Scientific Series on Meteorology of East Asia, vol. 3. World Scientific Publishing Company 9789812387042.

Li, Q., Jiang, J.H., Wu, D.L., Read, W.G., Livesey, N.J., Waters, J.W., Zhang, Y., Wang, B., Filipiak, M.J., Davis, C.P., Turquety, S., Wu, S., Park, R.J., Yantosca, R.M., Jacob, D.J., 2005. Convective outflow of south Asian pollution: a global CTM simulation compared with EOS MLS observations. Geophys. Res. Lett. 32, L14826. http://dx.doi.org/10.1029/2005GL022762.

Li, Z., Chen, H., Cribb, M., Dickerson, R., Holben, B., Li, C., Lu, D., Luo, Y., Maring, H., Shi, G., Tsay, S.C., Wang, P., Wang, Y., Xia, X., Zheng, Y., Yuan, T., Zhao, F., 2007. Preface to special section on east asian studies of tropospheric aerosols: an international regional experiment (EAST-AIRE). J. Geophys. Res. 112, D22S00. http://dx.doi.org/10.1029/2007JD008853.

Morys, M., Mims, F.M., Anderson, S.E., 2001. Design, calibration and performance of MICROTOPS II hand-held ozonometer. J. Geophys. Res. 106 (D13), 14573–14582.

Moorthy, K.K., Satheesh, S.K., Murthy, B.V.K., 1997. Investigations of marine aerosols over tropical Indian Ocean. J. Geophys. Res. 102, 18 827–18 842.

Moorthy, K.K., Babu, S.S., Satheesh, S.K., 2005. Aerosol characteristics and radiative impacts over the Arabian sea during the inter monsoon season: results from ARMEX field campaign. J. Atmos. Sci. 62 (1), 192–206.

Moorthy, K.K., Babu, S.S., Satheesh, S.K., 2007. Temporal heterogeneity in aerosol characteristics and the resulting radiative impact at a tropical coastal station-Part 1: microphysical and optical properties. Ann. Geophys. 25, 2293–2308.

Moorthy, K.K., Satheesh, S.K., Babu, S.S., Dutt, C.B.S., 2008. Integrated campaign for Aerosols, gases and Radiation Budget (ICARB): an overview. J. Earth Syst. Sci 117 (S1), 243–262.

Moorthy, K.K., Beegum, S.N., Babu, S.S., Smirnov, A., Rachel, J.S., Kumar, K.R., Narasimhulu, K., Dutt, C., Nair, V.S., 2010. Optical and physical characteristics of Bay of Bengal Aerosols during W_ICARB: spatial and vertical heterogeneities in the MABL and in the vertical column. J. Geophys. Res. 115, D24213. http://dx.doi.org/10.1029/2010JD014094.

Moorthy, K.K., Sreekanth, V., Chaubey, J.P., Gogoi, M.M., Babu, S.S., Kompalli, S.K., Bagare, S.P., Bhatt, B.C., Gaur, V.K., Prabhu, T.P., Singh, N.S., 2011. Fine and ultra fine particles at near free-tropospheric environment over the high altitude station Hanle, in trans- Himalayas: new particle formation and size distribution. J. Geophys. Res. 116, D20212. http://dx.doi.org/10.1029/2011JD016343.

Moorthy, K.K., Babu, S.S., Manoj, M.R., Satheesh, S.K., 2013. Buildup of aerosols over the Indian region. Geophys. Res. Lett. 40, 1011–1014. http://dx.doi.org/10.1029/2012GL054876.

Mishra, M.K., Rajeev, K., Thampi, B.V., Parameswaran, K., Nair, M., 2010. Micro pulse lidar observations of mineral dust layer in the lower troposphere over the south-west coast of Peninsular India during the Asian summer monsoon season. J. Atmos. Sol. Terr. Phys. 72, 1251–1259.

Nair, V.S., Moorthy, K.K., Alappattu, D.P., Kunhikrishnan, P.K., George, S., Nair, P.R., Babu, S.S., Abish, B., Satheesh, S.K., Tripathi, S.N., Niranjan, K., Madhavan, B.L., Srikant, V., Dutt, C.B.S., Badarinath, K.V.S., Reddy, R.R., 2007. Wintertime aerosol characteristics over the Indo-Gangetic Plain (IGP): impacts of local boundary layer processes and long-range transport. J. Geophys. Res. 112, D13205. http://dx.doi.org/10.1029/2006JD008099.

Nakajima, T., Sekiguchi, M., Takemura, T., Uno, I., Higurashi, A., Kim, D., Sohn, B.J., Oh, S.N., Nakajima, T.Y., Ohta, S., Okada, I., Takamura, T., Kawamoto, K., 2003. Significance of direct and indirect radiative forcings of aerosols in the East China Sea region. J. Geophys. Res. 108 (D23), 8658. http://dx.doi.org/10.1029/2002JD003261.

Nakajima, T., Yoon, S.C., Ramanathan, V., Shi, G.Y., Takemura, T., Higurashi, A., Takamura, T., Aoki, K., Sohn, B.J., Kim, S.W., Tsuruta, H., Sugimoto, N., Shimizu, A., Tanimoto, H., Sawa, Y., Lin, N.H., Lee, C.T., Goto, D., Schutgens, N., 2007. Overview of the atmospheric brown cloud East Asian regional Experiment 2005 and a study of the aerosol direct radiative forcing in East Asia. J. Geophys. Res. 112, D24S91. http://dx.doi.org/10.1029/2007JD009009.

Niranjan, K., Madhavan, B.L., Sreekanth, V., 2007. Micro pulse lidar observation of high altitude aerosol layers at Visakhapatnam located on the east coast of India. Geophys. Res. Lett. 34, L03815. http://dx.doi.org/10.1029/2006GL028199.

Pathak, B., Kalita, G., Bhuyan, K., Bhuyan, P.K., Moorthy, K.K., 2010. Aerosol temporal characteristics and the resulting impact on radiative forcing at a location in the northeast India. J. Geophys. Res. 115, D19204. http://dx.doi.org/10.1029/2009JD013462.

Pathak, B., Bhuyan, P.K., Gogoi, M.M., Bhuyan, K., 2012. Seasonal heterogeneity in aerosol types over Dibrugarh-North-Eastern India. Atmos. Environ. 47, 307–315. http://dx.doi.org/10.1016/j.atmosenv.2011.10.061.

Pathak, B., Borgohain, A., Bhuyan, P.K., Kundu, S.S., Sudhakar, S., Gogoi, M.M., Takemura, T., June 2014. Spatial heterogeneity in near surface aerosol characteristics across the Brahmaputra valley. J. Earth Syst. Sci. 123 (4), 651–663.

Podgorny, I.A., Ramanathan, V., 2001. A modeling study of the direct effect of aerosols over the tropical Indian Ocean. J. Geophys. Res. 106 (D20), 24097–24105.

Rahul, P.R.C., Bhawar, R.L., Ayantika, D.C., Panicker, A.S., Safai, P.D., Tharaprabhakaran, V., Padmakumari, B., Raju, M.P., 2014. Double blanket effect caused by two layers of black carbon aerosols escalates warming in the Brahmaputra River Valley. Sci. Rep. 4, 1–7. http://dx.doi.org/10.1038/srep03670, 3670.

Ramana, M.V., Ramanathan, V., Podgorny, I.A., 2004. The direct observations of large aerosol radiative forcing in the Himalayan region. Geophys. Res. Lett. 31, L05111. http://dx.doi.org/10.1029/2003GL018824.

Ricchiazzi, P., Yang, S., Gautier, C., Sowle, D., 1998. SBDART: a research and teaching software tool for plane-parallel radiative transfer in the earth's atmosphere. Bull. Am. Meteorol. Soc. 79, 2101–2114.

Satheesh, S.K., Moorthy, K.K., Babu, S.S., Vinoj, V., Dutt, C.B.S., 2008. Climate implications of large warming by elevated aerosol over India. Geophys. Res. Lett. 35, L19809. http://dx.doi.org/10.1029/2008GL034944.

Satheesh, S.K., Vinoj, V., Moorthy, K.K., 2010. Radiative effects of aerosols at an urban location in southern India: observations versus model. Atmos. Environ. 44, 5295–5304.

Sharma, A.R., Kharol, S.K., Badarinath, K.V.S., 2009. Satellite observations of unusual dust event over north-east India and its relation with meteorological conditions. J. Atmos. Sol. Terr. Phys. 71, 2032–2039.

Takami, A., Miyoshi, T., Shimono, A., Kaneyasu, N., Kato, S., Kajii, Y., Hatakeyama, S., 2007. Transport of anthropogenic aerosols from Asia and subsequent chemical transformation. J. Geophys. Res. 112 (D22). http://dx.doi.org/10.1029/2006JD008120.

Ward, J.H., 1963. Hierarchical grouping to optimize an objective function. J. Am. Stat. Assoc. 58, 236–244.

Winker, D.M., Hunt, W.H., McGill, M.J., 2007. Initial performance assessment of CALIOP. Geophys. Res. Lett. 34, L19803. http://dx.doi.org/10.1029/2007GL030135.

Zarzycki, C.M., Bond, T.C., 2010. How much can the vertical distribution of black carbon affect its global direct radiative forcing? Geophys. Res. Lett. 37 (20), L20807.